

Final Draft
of the original manuscript:

Keppler, J.K.; Martin, D.; Haramus, V.M.; Berton-Carabin, C.; Nipoti, E.;
Coenye, T.; Schwarz, K.:

**Functionality of whey proteins covalently modified by allyl
isothiocyanate. Part 1 physicochemical and antibacterial
properties of native and modified whey proteins at pH 2 to 7**

In: Food Hydrocolloids (2016) Elsevier

DOI: 10.1016/j.foodhyd.2016.11.016

1 **Functionality of whey proteins covalently modified by the cabbage compound allyl**
2 **isothiocyanate.**

3 **Part 1.**

4 **Physicochemical and antibacterial properties of native and modified whey proteins at**
5 **pH 2 to 7**

6
7 **Highlights**

- 8 • Whey protein isolate was covalently modified with allyl isothiocyanate
- 9 • The adducts showed increased hydrophobicity at pH 2, 4 and 6
- 10 • The protein β -sheet content increased
- 11 • Interfacial tension was reduced
- 12 • Antimicrobial activity of WPI was not significantly influenced

13
14
15 **Chemical compounds studied in this article**

16 Allyl isothiocyanate (PubChem CID: 5971), beta-Lactoglobulin (PubChem CID: 142-148)

17
18
19 **Abbreviations**

20 ACN, acetonitrile; ALA, α -lactalbumin; ANS, 8-anilinonaphthalene-1-sulfonic acid; AITC,
21 allyl isothiocyanate; ATR-FT-IR, attenuated total reflection Fourier-transform-infrared-
22 spectroscopy; A.U., arbitrary units; BSA, bovine serum albumin; DLS, dynamic light
23 scattering; E'_d , dilatational elastic modulus; E''_d , dilatational viscous modulus; FD, freeze
24 dried; FSD, Fourier self-deconvolution; GC, gas chromatography; IEP, isoelectric point; IFT,
25 indirect Fourier Transform; β -LG, β -lactoglobulin; MIC, Minimum inhibitory concentration;
26 n.tr.b., normalized to transmitted beam; P, protein; RT, retention time; SAXS, small angle X-
27 ray scattering; TFA, trifluoroacetic acid; WPI, whey protein isolate.

28
29
30

31 **Abstract**

32 Whey protein isolate (WPI) (~70 % β -lactoglobulin (β -LG)) is frequently used in foods as
33 natural emulsifying agent; however, at an acidic pH-value its emulsification capacity is
34 strongly reduced. The covalent attachment of natural electrophilic hydrophobic molecules to
35 WPI proteins is a promising method to change the physicochemical properties of WPI in
36 favour of a higher functionality at acidic pH.

37 In the present study different concentrations of the cabbage compound allyl isothiocyanate
38 (AITC) were covalently bound to WPI, and the related changes in physicochemical properties
39 (charge, aggregation, surface hydrophobicity and secondary structure) were monitored over a
40 wide pH range (pH 2 to 7). Additionally, the antibacterial activity before and after AITC
41 modification against different strains of *S. aureus* and *E. coli* was assessed.

42 The results showed that both whey proteins β -LG and α -lactalbumin (ALA) were modified by
43 AITC. This modification remained stable during pH adjustment. Unbound AITC was
44 successfully removed by the lyophilization process, which reduced the strong odour of the
45 volatile AITC. The hydrophobicity of the modified WPI increased significantly and the
46 protein's secondary and tertiary structure was altered. A shift of the isoelectric point towards
47 acidic conditions was observed. The interfacial tension at acidic pH-values 2 and 4 was
48 significantly reduced. These effects were less pronounced at pH 6 and 7. The relatively mild
49 antibacterial effect of native WPI was not significantly influenced by addition of AITC.

50 Thus, a higher surface activity of the AITC-modified WPI at acidic pH compared to native
51 WPI was evident, mediated by increased hydrophobicity of the WPI as well as increased
52 protein backbone flexibility.

53

54

55

56

57

58

59

60

61

62

63

64

65

66 1. Introduction

67 Commercial whey protein isolate (WPI) is used in various dispersions in food, feed or
68 cosmetic industry due to its foaming and emulsifying capacity (Dickinson, 2001; Gulzar,
69 Lechevalier, Bouhallab, & Croguennec, 2012; Lam, Ricky & Nickerson, 2015). The main
70 protein in WPI is β -lactoglobulin (β -LG) which is a globular amphiphilic molecule
71 comprising 162 amino acids and one sulfhydryl group partially buried. Its surface activity is
72 mainly mediated by adsorbing at an oil/water or air/water interface followed by partial
73 unfolding and alignment of hydrophobic residues towards the oil or air phase (Dickinson,
74 1999, 2001; Zhai et al., 2011). A smaller fraction of proteins in WPI consists of α -lactalbumin
75 (ALA), which has 123 amino acid residues (Brew, Castellino, Vanaman, & Hill, 1970) and
76 has a lower emulsifying capacity. To further enhance the surface activity of whey proteins
77 like β -LG the physicochemical properties are often changed by inducing high pressure or
78 thermal treatment – leading to partial or complete unfolding of the protein whereupon buried
79 hydrophobic amino acid residues get access to the surface and protein backbone flexibility
80 increases. However, depending on the protein concentration and energy input, the unfolding
81 can subsequently lead to protein aggregation and cross-linking through reactive thiol groups,
82 which then negatively affects the flexibility and surface activity of the protein (Lam
83 & Nickerson, 2015). Another method to modify the surface activity is the esterification of β -
84 LG with alcohols, which increases the hydrophobicity and flexibility of the protein and was
85 found to increase the emulsifying capacity of β -LG at acidic pH (Halpin & Richardson, 1985;
86 Sitohy, Chobert, & Haertlé, 2001).

87 A novel approach to influence the functionality of proteins is the covalent addition of an
88 electrophilic plant compound (Rade-Kukic, Schmitt, & Rawel, 2011; Keppler et al., 2014a;
89 Keppler, Koudelka, Palani, Tholey, & Schwarz, 2014b). Natural compounds that are known
90 to form covalent adducts with thiols and amines are organosulfur thiosulfinates (from *allium*)
91 (Wilde, Keppler, Palani, & Schwarz, 2016a, 2016b, Wilde et al., 2016c) and thiocyanates
92 (from *brassica*) (Keppler et al., 2014a; Keppler et al., 2014b; Rade-Kukic et al., 2011), as
93 well as α,β -unsaturated aldehydes (from *cinnamomum*) (Björkman, 1973; Kawakishi &
94 Kaneko, 1987; Murthy & Rao, 1986a; Rawel, Kroll, & Schröder, 1998). Such compounds
95 readily interact with deprotonated amine and/ or thiol groups of proteins at elevated pH (> 8).
96 The isothiocyanate allyl isothiocyanate (AITC) can be found in broccoli, cauliflower, Brussels
97 sprouts, cress and cabbage and is produced by the enzyme myrosinase through hydrolysis of
98 glucosinolate sinigrin upon damaging of plant cells (Fimognari, Turrini, Ferruzzi, Lenzi, &

99 Hrelia, 2012; Palani et al., 2016). All isothiocyanates have the R-N=C=S functional group in
100 common. The electrophilic C-atom forms thiocarbamoyl adducts with thiols, or thiourea
101 adducts with amines (Nakamura, Kawai, Kitamoto, Osawa, & Kato, 2009). The AITC
102 conjugation is a time, pH-value and concentration dependent reaction: the α -amino group of
103 lysine 1 and ϵ -amino group residues of leucines of β -LG are primarily reacting with AITC at
104 elevated pH upon deprotonation (Hanschen et al., 2012; Nakamura et al., 2009). The AITC
105 reaction with amino acid residues of β -LG was found to be controllable to a certain degree by
106 changing the protein/AITC ratio, revealing the n-terminal part of the protein as most reactive
107 (Keppler et al., 2014a; Keppler, et al., 2014b).

108 The covalent modification of milk protein β -LG by AITC was previously described in detail
109 (Keppler et al., 2014a; Keppler et al., 2014b; Rade-Kukic et al., 2011): The addition of AITC
110 to β -LG influenced the proteins folding, structure and consequently its physicochemical
111 properties – for example β -LG was found to interact positive-cooperatively with AITC –
112 resulting in a loosening of the protein folding (Keppler et al., 2014a). A higher flexibility, as
113 well as the attachment of hydrophobic residues could increase the amphiphilic character of
114 whey proteins and may potentially change the emulsifying capacity, especially in acidic
115 environment, where structural rigidity of β -LG reduces its surface activity.

116 In order to further understand the functionality of AITC-protein complexes, the covalent
117 modification of WPI with AITC and its influence on protein physicochemical properties were
118 studied over a wide pH range (i.e. pH 2, 4, 6 and 7). WPI was chosen instead of pure β -LG as
119 it is commonly used in food industry. Fresh prepared, as well as freeze dried WPI and WPI-
120 AITC conjugates were characterized for their interaction behaviour, followed by analyses of
121 charge (zeta potential), aggregation (dynamic light scattering), surface hydrophobicity (ANS
122 fluorescence), interfacial properties (drop tensiometer) and secondary/tertiary structure (ATR-
123 FT-IR). Additionally, the antibacterial effect of the modified WPI was assessed in comparison
124 to that of unmodified WPI. Effects of the AITC modification on emulsifying capacity of WPI
125 in o/w emulsions at pH 2, 4, 6 and 7 will be described in detail in another study.

126

127

128

129

130 2. Materials and Methods

131 2.1. Materials

132 All chemicals were of analytical grade: Allyl isothiocyanate (AITC >95 %) and 8-anilino-1-
133 naphthalenesulfonate (ANS) were obtained from Sigma Aldrich (Seelze, Germany), whey
134 protein isolate (WPI) (BiPRO, Davisco Foods International, Inc., Eden Prairie, US) with
135 97.7% protein and 75% β -LG in dry matter was used for modification.

136 2.2 Sample preparation

137 **2.2.1. Covalent modification.** 25 g L⁻¹ WPI was solved in MilliQ water for several hours to
138 assure complete hydration. All denatured proteins were removed by setting the pH-value to
139 4.6 with 3 M HCl. After 1 hour equilibration the samples were centrifuged (2000 *g, 5 min)
140 to remove precipitated (i.e. denatured) protein. The supernatant was filtered and set to pH 9
141 using 1 M NaOH. AITC modification was conducted at room temperature in 4 different
142 concentrations: 0.5 g L⁻¹, 1 g L⁻¹, 2 g L⁻¹ or 3 g L⁻¹ w/w per 25 g L⁻¹ WPI (i.e. 0.2 g L⁻¹, 0.4 g
143 L⁻¹, 0.8 g L⁻¹ and 1.2 g L⁻¹ per 10 g L⁻¹ WPI). These concentrations correspond to an
144 approximate molar ratio of 1:3, 1:6.5, 1:13 and 1:20 M proteins per M AITC. The respective
145 amount of AITC was directly added to the protein solution (ca. 10 to 15 minutes after setting
146 the pH-value to 9) and stirred over night at room temperature to assure complete binding as
147 described by Keppler et al., (2014a). The high pH value 9 was chosen to assure deprotonation
148 of free amine and thiol groups, so that a binding reaction with AITC is possible. The addition
149 and binding reaction of AITC directly caused a decrease of the pH-value (to a final pH of ~7
150 after complete binding); preventing base denaturation of the proteins, which was found to
151 partly occur after 10 h stirring at pH 9 (Boye, Ismail, & Alli, 1996).

152

153 **2.2.2. Lyophilization.** The samples were set to pH 7 and lyophilized to remove any unbound
154 AITC and termed “modified”. Additionally, WPI, which was subjected to the same
155 precipitation process as described above, but without addition of AITC was also freeze dried,
156 to act as reference material as “native” WPI. For lyophilisation, all samples were frozen at -20
157 °C (to prevent cold denaturation) for 24 h and freeze dried using a laboratory freeze dryer
158 (Gamma 1-16 LSCplus, Martin Christ Gefriertrocknungsanlagen GmbH, Osterode, Germany)
159 and then stored in tightly sealed flasks at 0 °C in the dark until further use. The concentration
160 of remaining AITC in the modified WPI samples after the lyophilization process was
161 determined by headspace GC as described below. For this 50 g L⁻¹ of the modified WPI was

162 dissolved in 1 ml Milli Q water directly inside the closed GC vials for at least 2 h, before the
163 analysis.

164

165 **2.3. Analysis of the covalent interaction between AITC and WPI**

166 **2.3.1. Analysis of AITC binding by HPLC.** 1 g L⁻¹ native or AITC-modified freeze dried WPI
167 at pH 7 was dissolved in Milli Q water and analyzed by RP-HPLC as described by Keppler et
168 al. (Keppler, Sönnichsen, Lorenzen & Schwarz, 2014c) using an Agilent 1100 Series HPLC
169 with a diode-array detector and PLRP-S column (300 Å, 8 µm, 150 x 4.6 mm, Agilent
170 Technologies, Santa Clara, USA). The injection volume was 20 µl at a flow rate of 1.0 ml/min
171 and a column temperature of 40 °C using eluents A (0.1% (v/v) TFA in water) and B (0.1%
172 TFA (v/v) in ACN). The elution used gradient steps of 35-38% B (1-8 min), 38-42% B (8-16),
173 42-46% B (16-22 min), 46-100% B (22-22.5 min) and 100-35% B (23-23.5 min). The
174 detection wavelength was 205 nm. Standards and calibrations of pure β-LG AB, as well as
175 ALA and BSA were run.

176

177 **2.3.2. Analysis of AITC by headspace gas chromatography.** Before the lyophilisation
178 process several ml of each modified WPI at pH 7 were put aside for binding analysis in
179 Headspace GC and termed “bound”, as they represented the modified WPI. Additionally to
180 these samples, WPI samples with “unbound” AITC were prepared as reference. For this, the
181 WPI supernatant was set to pH 7 instead of pH 9, before addition of the same concentrations
182 of AITC as described above. These samples were not stirred overnight, as at these conditions
183 no binding occurred. The fraction of protein-bound AITC after protein modification was
184 determined mathematically by subtracting the concentration of free AITC in the “bound”
185 sample from concentration of free AITC in the “unbound” sample. Both concentrations were
186 determined by headspace-GC as described by Keppler et al. (2014a). Briefly: All samples
187 were diluted to 10 g L⁻¹ protein and 1 ml of the samples were filled into headspace vials (20
188 ml) and incubated at 65 °C for 15 min prior to injecting 0.2 ml of the sample loop fill from the
189 HP7694 headspace auto sampler to the GC HP 6890 (Agilent Technologies, Böblingen). The
190 GC was equipped with a FID and the column was a DB-1701 column (Agilent J & W, 30 m x
191 0.321 mm), coated with a low-to mid-polar phase (bonded and cross-linked, 14%-
192 Cyanopropyl-phenyl (-o-methylpolysiloxane)). Oven temperature was programmed from 45
193 °C, 7 min to 220 °C in 30 °C steps and with 3 min holding time. A split ratio of 2:1 was used
194 and the split flow of the carrier gas was 2 ml/min. A calibration was conducted in triplicate by
195 using different concentrations of AITC dissolved in MilliQ water, without protein addition.

196 **2.4. Surface hydrophobicity by ANS**

197 The hydrophobicity was measured as described in Lam & Nickerson (2015) using the external
198 fluorescence probe 8-anilino-1-naphthalenesulfonate (ANS). Freeze-dried native or AITC-
199 modified WPI (Modification: 0.4 g L⁻¹ AITC per 10 g L⁻¹ WPI) were adjusted to pH 2, 4, 6 or
200 7 before the final concentration was set to 0.3, 0.4, 0.5 and 0.6 g L⁻¹ and again controlled for
201 pH-stability. 20 µl of 8 mmol L⁻¹ ANS in water, adjusted to the respective pH of the WPI, was
202 added to 1.6 mL protein solution, vortexed and stored in the dark for 5 min. For control,
203 proteins without ANS were used and the blank was ANS in water without protein at the
204 respective pH-value. The fluorescence was measured at 390 nm excitation and 490 nm
205 emission wavelengths, using 2.5 nm slit width for all samples (and additionally a 5 nm slit
206 width for pH 6 and 7 samples) and a 1 cm quartz cuvette with 4 polished sides on a Varian
207 Cary eclipse fluorescence spectrometer (Varian Australia PTY, Ltd.). The net fluorescence
208 intensity was calculated by subtracting the control samples from the protein samples with
209 ANS at each protein concentration. The ANS fluorescence in dependence of the protein
210 concentration gave a straight line. The slope served as hydrophobicity index. All samples
211 were measured in triplicate.

212

213 **2.5. Influence of AITC binding on zeta potential and aggregation**

214 **2.5.1. Zeta potential and dynamic light scattering**

215 Zeta potential and particle size by dynamic light scattering were measured using a Zetasizer
216 nano ZS (Malvern Instruments GmbH, Herrenberg, Germany). WPI, native or AITC-modified
217 with AITC (Modification: 0.4 g L⁻¹ AITC per 10 g L⁻¹ WPI) and freeze dried at pH 7 was
218 dissolved in demineralized water for at least 1 h and either measured directly or adjusted to
219 pH 2, 4 or 6 using 1 M HCl. The WPI concentration was set to 10 g L⁻¹ and all samples were
220 filtered through a 0.2 µm syringe filter to remove dust. For zeta-potential measurements, the
221 solutions at pH 2, 4, 6 and 7 were filled in clear disposable zeta cells (DTS1060C), which
222 were previously rinsed with ethanol and then cleaned with water. The equilibration time was
223 120 s; the dielectric constant was 78.5 and viscosity 0.8872 cP. To determine the isoelectric
224 point (IEP) of native and modified WPI the pH-value of the solutions was slowly reduced by
225 adding droplets of 0.1 M HCL and confirming the pH-value.

226 For dynamic light scattering (DLS) 1 ml of the filtered WPI solutions at pH 2, 4, 6 or 7 were
227 carefully pipetted into quartz cuvettes with square aperture and 4 clear sides to prevent any
228 foaming. Measurements were conducted using 173 ° backscatter and a refractive index of

229 1.45 for protein. All measurements were performed at 20 °C and measurements were done at
230 least in triplicate.

231 **2.5.2. Small angle x-ray scattering**

232 SAXS experiments were performed at the BioSAXS Beamline P12 at PETRA III
233 (EMBL/DESY, Hamburg, Germany). The energy of X-ray beam was 10 keV and the beam
234 size 0.1 mm (V) × 0.2 mm (H). Sample to detector distance was 3.1 m and the q -range 0.03 to
235 4 nm^{-1} . Scattering patterns were measured using Pilatus 2M pixel detector. The samples (of
236 approximately 20 μl volume) were injected into the sample cuvette using an automated liquid
237 handling sample changer. In order to reduce the risk of the radiation damage the sample was
238 moved slightly during the exposure. The temperature was 20 °C. For each measurement, we
239 recorded 20 diffraction patterns originating from the same sample volume, using an exposure
240 time of 0.045 s per frame. Before and after each SAXS measurement from the sample, a
241 signal from H₂O was measured and used for background subtraction. The background-
242 corrected SAXS data were used to calculate one-dimensional scattering curves by angular
243 averaging. The data were corrected for transmitted beam. In order to verify that no artifacts
244 had occurred as a result of radiation damage, all scattering curves for a recorded dataset were
245 compared to a reference curve (typically the first exposure) before being integrated using an
246 automated acquisition and analysis program (Franke, Kikhney, & Svergun, 2012). The range
247 of the reciprocal space vector q was calibrated using diffraction patterns of silver behenate
248 (Blanton, T.N., Barnes, C.L., Lelental, M., 2000).

249 **2.6 Fourier-Transform-Infrared-Spectroscopy (FT-IR) using attenuated total reflection** 250 **(ATR) measuring cell**

251 The FT-IR measurements were performed with a Tensor 27 spectrometer (Bruker Optics,
252 Ettlingen, Germany). The measurements were carried out in the mid-infrared, i.e. in the wave
253 number range 4000-900 cm^{-1} . For the detection a LN-MCT Photovoltaic detector (Bruker
254 Optics), cooled with liquid nitrogen, was used. The spectrometer specific software OPUS
255 Version 65 (Bruker Optics) was applied for recording of the spectra, for monitoring and
256 control of the spectrometer and the thermostat Haake DC 30 (K20) (Thermo Haake,
257 Karlsruhe, Germany). FT-IR was performed using a BioATR-II measuring cell at 25 °C. 180
258 scans were made per analysis.

259 10 g L^{-1} modified or unmodified lyophilized WPI at pH 2, 4, 6 or 7 was prepared in demin.
260 water, using 6 M or 1 M HCl, respectively. FT-IR measurements were conducted with these

261 protein solutions. All samples were corrected for demin. water. Based on the obtained spectra,
262 Fourier self-deconvolution (FSD) was performed with a resolution enhancement factor of 3.0
263 1/cm and a bandwidth (full width at half height) of 18 1/cm using software OPUS Version 65,
264 over the wavenumber range 1780-1480 cm⁻¹. The resulting bands in the amide I range (1730-
265 1590 cm⁻¹) were integrated for the calculation and quantification of the structural components.
266 In addition, 4th derivatives were calculated from the measured and corrected spectra with the
267 use of 9 smoothing points.

268 **2.7. Determination of the minimum inhibitory concentration**

269 Antimicrobial activity of modified and unmodified WPI, as well as of AITC against
270 *Escherichia coli* ATCC 8739, *Staphylococcus aureus* LMG 10147 and *S. aureus* Mu50 was
271 assessed by a broth microdilution method (Cockerill, 2012). All strains were grown
272 aerobically at 37°C on Tryptic Soy Agar (Oxoid, Drongen, Belgium). Inhibition of bacterial
273 growth was assessed using flat-bottomed 96-well microtiter plates (TPP, Trasadingen,
274 Switzerland). The inoculum was standardized at approx. 5 x 10⁵ colony forming units/ml of
275 Tryptic Soy Broth (Oxoid). Before adding bacteria, the pH of the growth medium was
276 adjusted with 1M HCl. The plates were incubated at 37°C for 24 h and the optical density was
277 determined at 590 nm using a multilabel microtiter plate reader (Envision Xcite, Perkin Elmer
278 LAS, Waltham, MA).

279 **2.8. Statistical analysis**

280 All results were expressed as arithmetic means and standard deviation of replicated analyses.
281 Data were analyzed by two-way ANOVA with Tukey's multiple comparison test at a 0.05-
282 level of significance. Statistics, as well as all figures were done using GraphPad Prism
283 (version 6.05, GraphPad Software, San Diego, USA).

284

285

286

287

288

289

290 3. Results & Discussion

291 3.1. Characterization of the covalent modification

292 The physicochemical properties of conjugates consisting of allyl isothiocyanate (AITC) and
293 whey protein isolate (WPI) were characterized in detail.

294

295 **3.1.1. High pressure liquid chromatography.** According to HPLC analysis the WPI used for
296 protein modification contained 75.7 ± 1.4 % β -lactoglobulin (β -LG) and 14.7 ± 0.1 % α -
297 lactalbumin (ALA) and < 4 % bovine serum albumin (BSA) and was completely native.

298 **Figure 1** shows the HPLC chromatogram of freeze dried native WPI and WPI modified with
299 different concentrations of AITC. The results indicate that the AITC modification occurred to
300 both genetic variants of β -LG present in WPI (β -LG A and B, retention times (RT) = 19.1 and
301 19.9 min) to a similar extent, and to a minor extent also to ALA (RT = 10.6 min). The
302 modified ALA (RT = 13.8 min) partly overlapped with the minor peak of residual BSA (RT =
303 13.7 min). The modified whey proteins became more hydrophobic – reflected in an increase
304 of the retention time (RT > 20 min). For β -LG the occurrence of several new peaks clearly
305 shows that the protein has several binding sites for AITC. It is assumed that the RT of the
306 protein correlates with the number of bound AITC molecules.

307

308 According to the chromatogram both proteins, β -LG and ALA, showed a binding reaction
309 with AITC – however, β -LG had multiple binding sites and ALA only approximately 1
310 binding site per M ALA. A maximum binding of β -LG was found to result in five bound
311 AITC molecules per β -LG molecule (Keppler et al., 2014a; Keppler et al., 2014b). The ALA
312 modification in WPI was expected as AITC was found to react with deprotonated amine- and
313 thiol groups of β -LG, i.e. cysteine, leucine and lysine residues (Keppler et al., 2014a; Keppler
314 et al., 2014b). AITC and other isothiocyanates were found to covalently interact at similar
315 binding sites with various proteins, like mustard 12S protein, soy protein, ovalbumin,
316 legumin, bovine serum albumin (Hernández-Triana, Kroll, Proll, Noack, & Petzke, 1996;
317 Kroll, Noack, Rawel, Kroeck, & Proll, 1994; Kroll, Rawel, Kröck, Proll, & Schnaak, 1994;
318 Murthy & Rao, 1986b; Rade-Kukic et al., 2011; Rawel et al., 1998; Vega-Lugo & Lim,
319 2009). Following this, the interaction of ALA with AITC as determined in **Figure 1** is
320 consistent with these findings.

321 A higher hydrophobicity of a protein-AITC conjugate compared to the unmodified protein
322 was also described by Rade-Kukic et al. (Rade-Kukic, Schmitt, & Rawel, 2011). Similarly,

323 Wilde et al. (2016a) found a higher hydrophobicity of β -LG-allycin and β -LG-diallyl disulfide
324 conjugates using the same HPLC method as described above. The insertion of a hydrophobic
325 molecule in the globular protein tends to reduce its hydrophilic surface patches.

326

327 **3.1.2. Gas chromatography (GC).** By determining the headspace/water equilibrium as
328 described by Keppler et al. (Keppler et al., 2014a) the binding of AITC to WPI can be
329 determined. The concentration of free AITC in the headspace is reduced exactly for the
330 amount of bound AITC in solution, allowing to calculate the bound AITC to a known protein
331 concentration. In a first experiment the stability of the AITC-WPI modification after adjusting
332 to the different pH-values (pH 2, 4, 6 and 7) was controlled and assessed by GC analysis
333 (results not shown). **Table 1** shows the concentration of free and WPI bound AITC after
334 adjusting the samples to pH 7: The results confirm that the AITC concentration in the
335 headspace of the WPI “unbound” samples corresponds to a concentration expected for
336 completely unbound AITC, whereas the “bound” samples showed the reduced amount of
337 AITC after interacting with the protein. The estimated molar concentration of covalently
338 bound AITC increased with increasing addition of AITC to the WPI (i.e. 1.19, 1.47, 1.62, 1.85
339 mM covalently bound after addition of 0.2, 0.4, 0.8 and 1.2 g L⁻¹ AITC to 10 g L⁻¹ WPI,
340 respectively). Since WPI is a mixture of β -LG and ALA, the bound AITC per mol protein is
341 given as sum of β -LG and ALA.

342

343 For freeze-dried WPI (“bound FD”) the free AITC concentration was reduced by
344 approximately one or two orders of magnitude (i.e. from 7.90E⁻² g L⁻¹ free AITC to 2.11E⁻³ g
345 L⁻¹ and from 0.249 to 7.75E⁻³ g L⁻¹, after addition of 0.2 and 0.4 g L⁻¹ AITC to 10 g L⁻¹ WPI,
346 and from 0.599 g L⁻¹ free AITC to 1.83E⁻² g L⁻¹ for 0.8 g L⁻¹ AITC addition), confirming that
347 the freeze drying process eliminated most of the unbound fraction of AITC from the sample.
348 The sample with the highest molar ratio of AITC showed only marginal free AITC far below
349 the detection limit, the reason for this is unknown. Removal of unbound allycin from
350 covalently modified WPI by freeze drying or spray drying was reported recently (Wilde et al.,
351 2016b). In accordance with the results from HPLC, an almost complete binding reaction
352 (saturation of binding sites) was visible for the molar ratio 1:24 with n = 3.2 [mol/mol]
353 binding sites. Assuming n = 5 binding sites for β -LG (Keppler et al., 2014a; Keppler et al.,
354 2014b; Rade-Kukic et al., 2011) and n = 1 binding site on ALA (**Figure 1**), the percentual
355 distribution of the proteins in the WPI (i.e. 75 % β -LG, 14 % ALA, < 4 % BSA) allows a
356 maximum of approximately 3.7 to 3.9 binding sites. In summary, it can be concluded that the

357 increasing addition of AITC to WPI resulted in an increase of AITC molecules covalently
358 bound to WPI proteins – confirming the results shown by HPLC in **Figure 1**. For the
359 following experiments a concentration of 0.4 g L⁻¹ AITC was chosen in order to achieve a
360 high β -LG modification rate without using excessive AITC. This concentration also allowed a
361 good removal rate of unbound AITC from the sample and the modification remained stable
362 after adjusting the pH-value to 2, 4, 6 or 7.

363

364 **3.2. Surface hydrophobicity by fluorescence probe ANS**

365 The influence of AITC modification on the surface hydrophobicity of WPI was further
366 analyzed by using freeze dried native “unmodified” or “modified” WPI with the anionic
367 fluorescence probe ANS (1-anilino-8-naphtalenesulfonate). ANS interacts with hydrophobic
368 patches on the protein surface through hydrophobic or electrostatic interactions (i.e. via ion
369 pairing of the negatively charged sulfonate groups of ANS with positively charged amino
370 acids of the protein (histidine, lysine, arginine), stabilized through van der Waals forces
371 (Hawe, Sutter, & Jiskoot, 2007)). The binding of ANS to a protein results in an increase of the
372 ANS fluorescence. Increased ANS binding correlates directly with increased hydrophobicity
373 of a protein.

374

375 The hydrophobicity index was higher at pH 2 and 4 (hydrophobicity index ~836 and ~507)
376 compared to pH 6 or 7 (~108 and ~129) (**Figure 2**). As the ANS fluorescence was very low at
377 pH 6 and 7, these measurements were repeated with a higher slit width of 5 nm, but the
378 difference between native and modified protein was still the same as in **Figure 2** (results not
379 shown). The pH-dependent fluorescence intensity of ANS is caused by the positive charge of
380 the proteins at acidic pH (compare zeta potential in **Figure 3**), which favours electrostatic
381 complexes of negatively charged ANS with the protein. Similarly, the low fluorescence at pH
382 6 and 7 is a result of the negative charge of the WPI. Therefore, a direct comparison of the
383 hydrophobicity index between the acidic and the neutral samples is not possible. However, the
384 AITC-modification increased the ANS binding to the protein at each pH-value tested
385 (hydrophobicity index ~ 919, ~600, ~164 and ~146 for pH 2, 4, 6 and 7 respectively) while
386 the zeta potential of the native and the modified WPI was not significantly different at similar
387 pH-values (with the exception of pH 6, see **Figure 3**). Additionally, the size of the native and
388 modified WPI did not significantly differ at pH 2, 6 and 7 (**Table 2**), so that protein
389 aggregation was not the cause for the differences in the ANS interaction between native and
390 modified WPI. Accordingly, the AITC modification resulted in a higher surface

391 hydrophobicity of the modified WPI. The increase of the hydrophobicity index at pH 2 is also
392 in accordance with the results from HPLC (**Figure 1**), where both eluents had a pH-value of ~
393 2 and the retention time of the modified protein increased with increasing AITC binding. This
394 increase of hydrophobicity could be caused by conformational differences between the native
395 and the modified WPI (**cross ref 3.4.**) and/or be directly mediated due to the incorporation of
396 hydrophobic AITC to the protein.

397 An intensification of the ANS fluorescence of WPI at acidic pH-value caused by stronger
398 binding effects is consistent with literature (Alizadeh-Pasdar & Li-Chan, 2000; Das &
399 Kinsella, 1989; Rade-Kukic et al., 2011). Further, a higher surface hydrophobicity index for
400 pH 4 of AITC modified β -LG was also described by Rade-Kukic et al., (2011).

401

402 **3.3 Aggregation and charge analysis**

403 *3.3.1. Dynamic light scattering and zeta potential*

404 The aggregation behaviour (based on the hydrodynamic radius (R_H)) of the AITC-modified
405 whey proteins at different pH-values is listed in **Table 2**; the corresponding zeta-potential is
406 visible in **Figure 3**. According to the volume weighted size distribution of the freeze dried
407 native WPI, a main fraction (peak I) comprised proteins with an increasing particle size from
408 1.55 nm at pH 2 (approx. 1 monomer), 2.13 nm at pH 4 (approx. 1-2 monomers), 2.98 nm at
409 pH 6 and 2.97 nm at pH 7 (both approx. 2 monomers). The percentage distribution of this
410 peak I fraction on the overall particle size was 100 % with the exception at pH 2, where a
411 bimodal size distribution was evident and a peak II fraction (0.32 % volume) with a particle
412 size of 9.44 nm occurred. This size corresponds to aggregates of approximately 250
413 monomers.

414

415 The observed R_H of WPI at pH 2 correlates well with the size of β -LG monomers reported in
416 literature (Majhi et al., 2006; Sawyer & Kontopidis, 2000). The low particle size of the native
417 WPI proteins at pH 2 was expected, since WPI consists mainly of β -LG (~75 %), which is
418 reported to be monomeric at pH 2 (Fogolari et al., 1998). At pH 6 and 7 native β -LG is known
419 to form mostly dimers (Gao et al., 2014; Keppler, Martin, Garamus, & Schwarz, 2015) –
420 explaining the higher particle size of peak I with approximately 2.98 nm.

421 With the exception of pH 4, the size of AITC-modified WPI was not significantly different
422 from that of native WPI. The main fraction sizes were 1.35 nm, 15.30 nm, 2.03 nm and 2.77
423 nm at pH 2, 4, 6 and 7, respectively. For the modified WPI, strong protein aggregation was
424 evident at pH 4, with a main fraction percentage of 79 %. A second size fraction (peak II) of

425 approximately 16 % consisted of aggregates > 150 nm and a third fraction (peak III) of 1 %
426 particles with > 2000 nm size occurred even in the filtered samples. As the samples exhibited
427 turbidity before filtration, larger particles than the pore size of the filter have been excluded.
428 The actual percentage distribution of these large particles is much higher than indicated here.

429

430 In contrast to the present results, where no significant size difference between native or
431 modified WPI was evident, we recently reported protein monomerization after AITC
432 modification of pure β -LG at pH 7 (Keppler et al., 2014). However, in the previous study
433 highly purified β -LG was used instead of WPI and the unbound AITC was not removed by
434 lyophilisation, which could be the cause for the differences in the determined size.

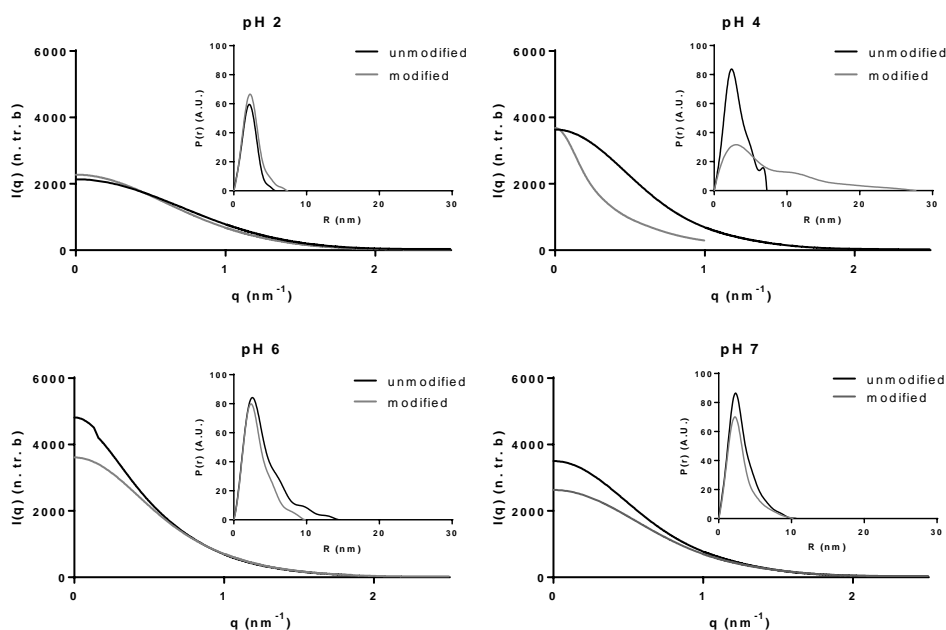
435 The observed aggregation and low solubility of the modified WPI at pH 4 can be explained by
436 its changed IEP after modification: The IEP (zeta potential of ~ 0 mV) was reduced from pH
437 ~ 4.99 for native WPI to pH ~ 4.68 for modified WPI (**Figure 3**). At pH 2 the zeta potential
438 increased to $\sim +25$ mV for both WPI, and decreased at pH 7 to ~ -25 mV. The IEP shift to a
439 more acidic pH-value can be explained by AITC binding to free amine groups – thereby
440 removing some positive charges from the overall charge of the protein. The addition of
441 negative charges to β -LG by phosphorylation or by blocking of positive charges was also
442 found to shift the IEP to more acidic pH-values (Sitohy, Chobert & Hertlé 1995). Pure β -LG
443 was reported to have an IEP of 5.2, and ALA an IEP between 4.1 and 4.8 (Hunt & Dalgleish,
444 1994). Therefore the results for the determined IEP of the native and the modified WPI are
445 consistent with literature.

446

447 **3.3.2. Small-Angle-X-Ray Scattering (SAXS)**

448 Experimental SAXS curves for native and modified WPI at pH 2, 4, 6 and 7 (**Figure 4**) were
449 analyzed by applying the Indirect Fourier Transform (IFT) method (Glatter, O. *J. Appl. Cryst.*
450 **1977**, *10*, 415-421.) using software GNOM (Svergun D.I., Semenyuk A.V., Feigin L.A.
451 (1988). *Acta Cryst.*, *A44*, 244-250). The resulting pair- distance distribution functions
452 ($p(r)$) are shown as small inserts in **Figure 4**. They describe the paired-set of all distances
453 between electrons in the protein. The maximum possible distance (D_{\max}) can be seen by the
454 intersection of the curves with the x-axis. All measurements were executed with 0.5 % and 1
455 % native and modified WPI at pH 2, 4, 6 and 7 to check the change of the protein structure
456 and interactions among proteins with increasing concentration; however the normalized by
457 protein concentration SAXS curves at intermediate and large q interval were similar for both
458 concentrations.

459 At pH 2 the native and modified WPI showed almost similar $p(r)$ functions, which almost
460 symmetrical form correlates well with a globular protein (Keppler, Martin, Garamus, &
461 Schwarz, 2015). The slightly higher $p(r)$, as well as R hints at a more unfolded globular
462 structure for the modified protein. At pH 4 the SAXS curves and $p(r)$ functions of the native
463 and the modified WPI differ significantly. Both functions for the native and the modified WPI
464 exhibited an increase in the pair distances hinting at aggregation, but the large R of the
465 modified WPI as well as the small increase at $R= 10$ nm hints at large elongated aggregates.
466 Precipitated modified WPI was visible at the bottom of the measuring tubes at pH 4, which
467 reveals that even larger protein aggregates were present. In contrast, the native WPI
468 aggregates were still rather spherical. At pH-value 6 the SAXS curves of the native and
469 modified WPI differed primarily in the scattering intensity ($I(q)$). The corresponding $p(r)$
470 functions revealed some elongated aggregates at pH 6 for the native WPI, which were not
471 observable for the modified WPI. The pair distance distribution functions of the native and
472 modified WPI at 7 reflect spherical proteins with a higher size compared to the WPI at pH 2.
473 The described SAXS curves and $p(r)$ functions clearly reflect the size changes of the WPI
474 observed in DLS (Table 2) at the different pH-values. The aggregation of the modified WPI at
475 pH 4 as well as the slight aggregation of the native WPI at pH 6 was caused by the different
476 IEPs of the native and the modified proteins (with the IEP of modified WPI nearer to pH 4
477 and the native nearer to pH 6). The smaller protein size reflected at pH 2 hints at monomeric
478 structures, whereas the protein sized at pH 7 were rather dimeric or trimeric.
479



480 **Figure 4** SAXS curves of 0.5 % native and modified WPI at pH 2, 4, 6 and 7. Small inserts show the
 481 corresponding $p(r)$ functions. I , intensity; q , scattering vector amplitude; n.tr.b, normalized to transmitted beam.
 482

483

484 The SAXS curves were analyzed for the apparent radius of gyration ($^{app}R_g$) [nm], the D_{max}
 485 required for the $p(r)$ functions and the possible molecular weight [kDa] of the aggregates
 486 (**Table 3**). As expected, the $^{app}R_g$ again reflects the protein aggregation at the respective IEP
 487 of the proteins: The native protein exhibited increasing protein sizes in the order pH 2 < pH 7
 488 < pH 4 < pH 6, whereas the $^{app}R_g$ of the modified WPI was in the order pH 2 < pH 7 < pH 6 <
 489 pH 4. The D_{max} was almost in similar order of the native and the modified WPI.

490 **Table 3.** Apparent radius of gyration, maximum distance, scattering intensity and R_g/R_H ratio for
 491 unmodified and modified WPI at pH 2, 4, 6 and 7.

pH value	Sample	Apparent radius of gyration ($^{app}R_g$) [nm]		Maximum distance (D_{max}) [nm]	Scattering intensity $I(0)$ [n. tr.b]		R_g/R_H
pH 2	unmodified	1.69	$\pm 0.1^a$	5.8	1788	$\pm 4.35^a$	1.08
	modified	1.95	$\pm 0.1^a$	7.5	2259	$\pm 5.46^b$	1.45
pH 4	unmodified	2.61	$\pm 0.1^a$	10	3667	$\pm 8.12^a$	1.16
	modified	5.76	$\pm 0.60^b$	29	4399	$\pm 28.91^b$	0.38
pH 6	unmodified	3.06	$\pm 0.1^a$	14.4	4670	$\pm 12.49^a$	1.03
	modified	2.44	$\pm 0.1^b$	9	3536	$\pm 12.87^b$	1.20

pH 7	unmodified	2.36	$\pm 0.1^a$	10	3598	$\pm 12.10^a$	0.79
	modified	2.19	$\pm 0.1^a$	10	2726	$\pm 13.83^b$	0.79

492

493 It can be concluded that the native WPI proteins in the present experiment were mostly
494 present as monomers at pH 2, with only some minor dimer fractions. The observed R_g of 1.69
495 nm listed in **Table 3** corresponds well with the R_g of ALA monomers at pH 2 (i.e. acid
496 molten globular structure with 17.2 Å (1.72 nm) (Kataoka, Kuwajima, Tokunaga, & Goto,
497 1997) or β-LG monomers at pH 2 (i.e. 1.52 nm (Verheul, Pedersen, Roefs, & Kruif, 1999)).
498 At pH 4 the size of the native WPI proteins in the present study increased to that of β-LG or
499 β-LG/ALA dimers or trimers. The R_g of a dimeric β-LG A in buffer pH 7 was reported to be
500 between ~2.1 nm (Panick, Malessa, & Winter, 1999) and 2.36 2.36 nm (Verheul, Pedersen,
501 Roefs, & Kruif, 1999), depending on the buffer system used. The high ^{app}R_g of native WPI at
502 pH 6 reflects some trimers, and the ^{app}R_g at pH 7 corresponds again to dimers. These results
503 are not only in accordance with literature but also verify the results obtained for the R_H by
504 DLS (**Table 2**).

505 The modified WPI has a higher ^{app}R_g at acidic pH 2 and 4 compared with the native WPI. The
506 reason could be that the WPI modification results in a more loose protein folding which
507 increases the R_g. Similar finding were reported for ALA, which R_g increased from 1.58 to
508 1.72 nm after forming a molten globule at pH 2 (Kataoka, Kuwajima, Tokunaga, & Goto,
509 1997). A molten globule like structure of the AITC modified β-LG was suggested at pH 4 by
510 CD measurements (Rade-Kukic, Schmitt, & Rawel, 2011). Additionally to that, the shifted
511 IEP of the modified WPI lowers the solubility at pH 4 and results in aggregation. At pH 6 and
512 7 the ^{app}R_g was in the range of β-LG or β-LG/ALA dimers, possibly some trimers. The results
513 are again in accordance with the size determination listed in **Table 2**.

514 Both the R_g (determined by SAXS) and the R_H (determined by DLS) are measures of protein
515 dimensions. The R_H reflects the size of a protein compared to a perfect sphere and contains
516 information on protein solvation, whereas the R_g gives information about the shape and
517 structure of a “dry” protein. The R_g/R_H ratio of native WPI was 1.08, 1.16, 1.03 and 0.79 for
518 pH values 2, 4, 6 and 7 respectively. The modified protein exhibited a higher ratio at pH 2 and
519 6 with 1.45 and 1.20. At pH 7 the ratio was similar to that of native WPI (i.e. 0.79). And near
520 the IEP at pH 4 the ratio was surprisingly low with 0.38. For a perfect sphere the R_g/R_H is
521 ~0.77 (Tande, Wagner, Mackay, Hawker, & Jeong, 2001) and a random coil polymer in a

522 good solvent has ~ 1.78 (Burchard, 1992). According to this interpretation the WPI
523 modification with AITC resulted in a more loose protein folding at pH 2 and 6. The protein
524 folding and solubility was not influenced at pH 7 and was relatively close to that of a globular
525 object. The low ratio near the IEP was probably caused by the high protein aggregation.
526 Similar observations with a R_g/R_H ratio below 0.77 were suggested to be caused by sample
527 impurities such as aggregates. These aggregates contribute strongly at the low q (large length
528 scale) of the DLS experiments, but not at the q -values (smaller length scale) from SAXS
529 analyses (Moitzi et al., 2011).

530

531 **3.4. Protein folding (ATR-FT-IR)**

532 **3.4.1. Amide I band.** Attenuated total reflection (ATR) Fourier transform infrared
533 spectroscopy (FT-IR) was used to analyse the protein folding in water at pH 2, 4, 6 and 7.
534 ATR was chosen due to the stability of the measuring cell at acidic conditions. **Table 4** lists
535 the mean % of distinct peak areas for band frequencies of the amide I region of native and
536 modified WPI, obtained by Fourier self-deconvolution of the measured and corrected spectra.
537 The amide I reflects mainly C=O stretching vibration of the peptide group and can be used to
538 assess the secondary structure of proteins (Pelton & McLean, 2000). For the present study a
539 simple model was used applying group frequency wavenumber around 1686 cm^{-1} for turns
540 and bends (Qi et al., 1997), 1658 cm^{-1} for alpha helical content and 1632 cm^{-1} for antiparallel
541 beta-sheet content (Fang & Dalglish, 1997)). The spectral peak intensity (positive or
542 negative) correlates with the respective content of the secondary structural element (Ioannou,
543 Donald, & Tromp, 2015). At pH 7 unmodified native WPI had approximately 21.31 % turns
544 and coils, 36.69 % alpha helix content and 42.0 % β -sheet concentration. The secondary
545 structure of native WPI was significantly influenced by the pH-value of the solution –
546 especially at pH 4, where a significant loss of beta-sheet content and increase of alpha helix
547 was evident. Further, a significant loss of coil and turns (1686 cm^{-1}) was also evident with
548 increasing acidity of the solution. The secondary structure of the modified WPI was
549 significantly altered from the native WPI in beta-sheet and alpha-helical content at all pH-
550 values – resulting in a markedly increase of beta-sheet structures in exchange of alpha-helix
551 content. This effect was especially evident at pH 7 and 6, and less so at pH 4 and 2.

552

553 According to literature, WPI at pH 7 was found to have 16 % alpha-helix, 33.6 % beta-sheet,
554 20.9 % turns and 29.6 % unordered structure (Rade-Kukic et al., 2011). Calculated without

555 unordered structure elements this would amount for 21.3 % alpha-helix, 44.8 % beta-sheet
556 and 27.8 % coils. The difference to the present results can be explained by the significantly
557 higher concentration of ALA in the WPI used (26.7 % instead of 4 %). At pH 4 an increase of
558 alpha-helical structure was reported after AITC modification of β -LG in exchange for beta-
559 sheet elements (Rade-Kukic et al., 2011). The increase of alpha-helical content at pH 4 was
560 also evident in the present results. However, in literature the AITC modification resulted in a
561 decrease of beta-strands at pH 7 – probably caused by dimer separation followed by partial
562 collapse of the beta-barrel (Rade-Kukic et al., 2011) - whereas in the present study the beta-
563 sheet content increased significantly with AITC modification. Further, according to DLS no
564 dimer separation was observed for the modified WPI – therefore the beta-barrel structure of β -
565 LG remained intact in the present study. This could be due to different measurement methods
566 applied (ATR-FT-IR versus circular dichroism), as well as due to different WPI used,
567 different AITC modification levels and due to the lyophilization step applied in the present
568 experiments. Additionally, Wilde et al. (2016c) also reported an increase of beta sheet
569 structure following the covalent modification of β -LG thiol group of WPI by allicin.

570

571 **3.4.1. Amide II and side chain absorption.** A list of signal maxima shifts in the amide II
572 region obtained after the 4th derivative of the spectra are summarized in (**Table 5**). Generally,
573 a shift from higher to lower wavenumber for the 1550 cm⁻¹ band frequency was observed after
574 modification of the WPI at all pH-values tested (i.e. from 1552 cm⁻¹ to 1548 cm⁻¹ at pH 2,
575 from 1551 cm⁻¹ to 1545 cm⁻¹ at pH 4, from 1551 cm⁻¹ to 1545 cm⁻¹ at pH 6 and from 1550 cm⁻¹
576 to 1549 cm⁻¹ at pH 7). A shift of amide II signals at 1550 cm⁻¹ towards a lower frequency
577 band generally correlates with increased β -sheet structure in proteins (Litvinov, Faizullin,
578 Zuev, & Weisel, 2012), which fits well with the present results of the amide I frequency band.
579 A second signal maximum at 1555 cm⁻¹, at 1557 cm⁻¹ or at 1556 cm⁻¹ was observed only for
580 the modified WPI at pH 2, 4 and 6 respectively, confirming conformational changes in the
581 amide II region (C-N). The appearance of a positive peak at 1555 cm⁻¹ after a covalent
582 modification of a protein amine group was also reported elsewhere (Almeida et al., 2014; Pan,
583 Cui, He, Gao, & Zhang, 2006). It is unclear why this 1555 cm⁻¹ signal maximum was not
584 observed in the modified protein at pH 7, since GC and HPLC results (**Table 1** and **Figure 1**)
585 confirm that the AITC modification occurred at all pH-values tested.

586

587 The 1517 cm⁻¹ frequency band increased from 1516.93 cm⁻¹ at pH 7 to 1517.62 cm⁻¹ at pH 6,
588 then decreased again to 1517.59 cm⁻¹ at pH 4. At pH 2 the band frequency was lowest with

589 1515 cm^{-1} . Although WPI is a rather complex sample with several signal overlay, these
590 specific signals could be caused by tyrosine. Tyrosine ring vibration in proteins is known to
591 occur approximately between 1515 cm^{-1} (Reinstädler, Fabian, Backmann, & Naumann, 1996)
592 to 1517 cm^{-1} (Ioannou et al., 2015) and a shift in its wavelength was found to reflect the local
593 environment of tyrosine. It can therefore be used as some kind of sensor for solvent
594 accessibility (Barth, 2007; Reinstädler et al., 1996). For example a change towards a lower
595 frequency band was correlated with a more lipophilic environment in a protein (Gaussier,
596 Lavoie, & Subirade, 2003) or reduced solvent exposure (Meersman, Smeller, & Heremans,
597 2002), which is similar to the frequency shift observed for native WPI at pH 2 in the present
598 study. At pH 7, where the tyrosine frequency of the native WPI was lowest, a beginning
599 deprotonation of the tyrosine residues could be possible (although the pKa of the tyrosines in
600 β -LG is around 10) (Barth, 2000). Following this the consecutive signal shifting to a lower
601 wavelength may indicate a more lipophilic microenvironment of tyrosine in native WPI at pH
602 2 (and to a minor extent also at pH 7), than at pH 4 and 6. These findings are consistent with
603 the results of a higher overall charge at pH 2 and pH 7 (**Figure 3**), resulting in a more rigid
604 globular protein folding especially at pH 2, thereby burying tyrosine in the hydrophobic core
605 of the globular protein and reducing its solvent accessibility. A lower backbone flexibility of
606 whey proteins at pH 2 is also consistent with its reduced emulsifying capacity at this pH-
607 value, hindering protein unfolding and interconnections and is also reflected in the
608 monomerization behaviour observed at this low pH-value (**Table 2**). Interestingly, the
609 described tyrosine frequency shift towards a lower frequency band at pH 2 was no longer
610 evident after protein modification. Here, the tyrosine vibration was lowest at pH 7 with
611 1515.44 cm^{-1} (showing strong hydrogen bonding) and increased to 1517.01 cm^{-1} at pH 6. A
612 further increase was observed at acidic pH 4 and 2 with 1517.82 cm^{-1} and 1517.81 cm^{-1} ,
613 respectively.

614

615 In comparison to the native WPI, the AITC modification shifted the possible tyrosine band
616 position towards lower wavenumbers at pH 7 and pH 6 and slightly towards a higher
617 wavelength number at pH 4. A significant increase of the band frequency was observed at pH
618 2 (increased solvent accessibility). The results at pH 2 and 4 could be evidence for a less rigid
619 protein folding of the modified WPI at these pH-values, increasing the contact of tyrosine
620 with water molecules. This is also partly reflected in the ANS fluorescence (**Figure 2**) which
621 was strongest at pH 2 and 4 after protein modification – suggesting that protein unfolding at
622 these pH-values increased the solvent accessibility of hydrophobic residues– thereby

623 increasing ANS binding to these patches. However, ANS binding was still higher in the
624 modified WPI at pH 6 (although less pronounced) and not significantly at pH 7; therefore the
625 hydrophobicity of the modified WPI was also mediated by the incorporation of hydrophobic
626 AITC molecules itself.

627

628 **3.6. Antibacterial activity**

629 **3.6.1. Antibacterial activity of native and modified WPI.** Given that the previous results
630 revealed altered physicochemical properties and surface activity of the AITC modified WPI, it
631 was of interest to evaluate the growth-inhibitory activity after WPI modification. The
632 minimum inhibitory concentrations (MIC) against different strains of Gram positive
633 bacterium *S. aureus* (Mu50 and LMG10147) and the Gram negative bacterium *E. coli* ATCC
634 8739 were evaluated using lyophilized unmodified or modified WPI (the residual amount of
635 unbound AITC in 1 % modified WPI solutions was below 0.015% (**Table 1**)). The
636 antibacterial activity was tested at pH-values 6 and 7, since at pH-values 2 and 4 the
637 microorganisms did grow poorly at best.

638 At pH-value 7 native WPI showed a mild effect on the growth of *E. coli* ATCC 8739 (0.68
639 A.U. to 0.41 A.U. reduction) and against *S. aureus* Mu50 (0.49 A.U. to 0.34 A.U.) at WPI
640 concentrations between 0.01 % and 4 % WPI (**Figure 5**).

641

642 The modification of WPI with AITC did not influence the antimicrobial activity of the WPI,
643 although this effect was not unequivocally visible for *E. coli* at pH 7. To verify this, the
644 antibacterial effect of WPI modified with 0.4 g L⁻¹ AITC (the same modification as used
645 above) or 1.2 g L⁻¹ AITC (complete modification) was compared to native WPI (**Figure 6**)
646 against *E. coli* strain ATCC 8739 at pH 7. The low activity of native WPI under these
647 conditions was confirmed (0.88 A.U. to 0.42 A.U. at concentrations between 0.004 % and 4
648 % WPI). In comparison, the activity of the modified WPI (both 0.4 and 1.2 g L⁻¹
649 modifications) against the *E. coli* strain tested was less pronounced than for the native WPI,
650 however this effect was less distinct for the 0.4 g L⁻¹ modification.

651

652 Mild growth inhibitory activity of pure β -LG against growth of Gram positive *S. aureus*
653 strains was already reported in literature (Chaneton, Pérez Sáez, J. M., & Bussmann, 2011),
654 which confirms the present results. On the other hand no effect of pure β -LG against resting
655 cells of *Pseudomonas fluorescens*, *Pseudomonas fragi* and *Bacillus subtilis* was observed
656 (Pan et al., 2007). Modifications of β -LG (i.e. acylation or amidation) reportedly increased its

657 antiviral or antimicrobial effect by incorporation of charged groups, e.g. antiviral properties
658 were reported after acylation of β -LG, caused by incorporation of strong negative charges into
659 the protein (Swart et al. 2009), whereas amidation (conversion of glutamate and aspartate
660 residues to asparaginy and glutaminy residues) increased the positive charge of the protein
661 which caused a strong bactericidal effect against resting cells of *Pseudomonas fluorescens*,
662 *Pseudomonas fragi* and *Bacillus subtilis*. A much weaker effect was also found against *E.*
663 *coli*, *Enterococcus faecalis*, *Salmonella typhimurium* and *Listeria monocytogenes* (Pan et al.,
664 2007).

665

666 **3.6.2. Antibacterial activity of AITC.** Although no antimicrobial effect of the protein bound
667 AITC was expected, the residual unbound AITC in the modified WPI (4% modified WPI
668 contained < 0.045 % free AITC) might still have antimicrobial activity. Therefore the activity
669 of pure AITC was evaluated without WPI at pH-values 6 and 7 (**Figure 7**). The results
670 confirm a strong growth-inhibitory effect of AITC against *E. coli* ATCC 8739 and *S. aureus*
671 *Mu50*, and a lesser effect against *S. aureus* LMG10147. The unbound AITC in the modified
672 WPI could therefore potentially have some growth inhibitory effect on *E.coli* and *S. aureus*
673 *Mu50* when using 4 % protein, however this is not clearly evident in **Figures 5** and **6**.

674

675 Similar to our results, a strong antimicrobial effect against a five strain mixture of *E. coli*
676 O157:H7 was reported for pure AITC solutions, although this effect was pH-dependent: the
677 MIC was 50 μ l/L at pH 6.5 (0.005 %) and 250 μ l/L at pH 7.5 (0.025 %) (Luciano & Holley,
678 2009). Antimicrobial activity of AITC against *E. coli* strains was also found by Mushantaf et
679 al. (Mushantaf, Blyth, & Templeton, 2012) in water and in refrigerated ground beef
680 (Muthukumarasamy, Han, & Holley, 2003). An antimicrobial effect of AITC against *S.*
681 *aureus*, *Pseudomonas aeruginosa* and *Listeria monocytogenes* was also reported and the
682 antibacterial mode of actions was suggested to be changed membrane properties of the
683 bacteria, resulting in potassium leakage and propidium iodide uptake (Borges et al., 2015).
684 The underlying mechanism is the interaction of the electrophilic C-atom in the R-N=C=S
685 group of AITC with surface components of the bacteria. Interestingly, the interaction of
686 bacteria membrane with AITC also changed the physicochemical properties of the membrane
687 (like increased hydrophobicity) (Borges et al., 2015). As this reaction occurs analogous to the
688 described electrophilic reaction of AITC with whey proteins (i.e. AITC is covalently bound to
689 proteins with its electrophilic C-atom), the protein bound AITC can no longer react with
690 bacteria components.

691

692 **4. Conclusion**

693 The present findings revealed that the covalent modification of WPI with AITC significantly
694 influenced the physicochemical properties of the WPI, especially at acidic pH: The surface
695 hydrophobicity increased strongly, the secondary structure was altered to more beta-sheet
696 components and signs of protein unfolding were evident. The IEP was shifted and the
697 interfacial tension at the oil/water interface was significantly lower compared to unmodified
698 WPI. The antimicrobial activity of WPI was not significantly influenced by AITC addition.
699 Following this, AITC modification of WPI could be a possible means to increase the surface
700 activity of WPI at acidic pH below the isoelectric point. A high emulsifying capacity of
701 AITC-modified WPI at acidic pH-value is conceivable.

702

703 **Acknowledgement**

704 This project was funded by the BMBF program FOCUS, TP 3.4 (LactoTrans). We are
705 grateful to Longina Reimann of the Max Rubner-Institute, Federal Research Institute of
706 Nutrition and Food, Department of Safety and Quality of Milk and Fish Products, Kiel,
707 Germany for the assistance with ATR-FT-IR measurements, to Heidrun Schwalowski and
708 Laura Müller of the Food Technology Division, CAU Kiel and to Clement Blanchet (EMBL)
709 at the P12 BioSAXS beamline.

710

711

712 **References**

- 713
- 714 Alizadeh-Pasdar, N., & Li-Chan, E. C. Y. (2000). Comparison of Protein Surface
715 Hydrophobicity Measured at Various pH Values Using Three Different Fluorescent
716 Probes. *Journal of agricultural and food chemistry*, 48(2), 328–334.
717 <http://dx.doi.org/10.1021/jf990393p>
- 718 Almeida, P. V., Shahbazi, M.-A., Mäkilä, E., Kaasalainen, M., Salonen, J., Hirvonen, J., &
719 Santos, H. A. (2014). Amine-modified hyaluronic acid-functionalized porous silicon
720 nanoparticles for targeting breast cancer tumors. *Nanoscale*, 6(17), 10377–10387.
721 doi:10.1039/c4nr02187h
- 722 Barth, A. (2000). The infrared absorption of amino acid side chains. *Progress in biophysics*
723 *and molecular biology*, 74(3-5), 141–173. doi:10.1016/S0079-6107(00)00021-3
- 724 Barth, A. (2007). Infrared spectroscopy of proteins. *Biochimica et Biophysica Acta (BBA) -*
725 *Bioenergetics*, 1767(9), 1073–1101. doi:10.1016/j.bbabi.2007.06.004
- 726 Benjamins, J., Cagna, A., & Lucassen-Reynders, E. H. (1996). Viscoelastic properties of
727 triacylglycerol/water interfaces covered by proteins. *Colloids and Surfaces A:*
728 *Physicochemical and Engineering Aspects*, 114, 245–254. doi:10.1016/0927-
729 7757(96)03533-9
- 730 Björkman, R. (1973). Interaction between proteins and glucosinolate isothiocyanates and
731 oxazolidinethiones from *Brassica napus* seed. *Phytochemistry*, 12(7), 1585–1590.
732 doi:10.1016/0031-9422(73)80372-3
- 733 Blanton, T.N., Barnes, C.L., Lelental, M. (2000). Preparation of silver behenate coatings to
734 provide low- to mid-angle diffraction calibration. *Applied Crystallography*. (33), 172–173.
- 735 Borges, A., Abreu, A. C., Ferreira, C., Saavedra, M. J., Simões, L. C., & Simões, M. (2015).
736 Antibacterial activity and mode of action of selected glucosinolate hydrolysis products
737 against bacterial pathogens. *Journal of Food Science and Technology*, 52(8), 4737–4748.
738 doi:10.1007/s13197-014-1533-1
- 739 Bos, M. A., & van Vliet, T. (2001). Interfacial rheological properties of adsorbed protein
740 layers and surfactants: a review. *Advances in Colloid and Interface Science*, 91(3), 437–
741 471. Retrieved from <http://www.sciencedirect.com/science/article/pii/S0001868600000774>
- 742 Boye, J. I., Ismail, A. A., & Alli, I. (1996). Effects of physicochemical factors on the
743 secondary structure of beta-lactoglobulin. *The Journal of dairy research*, 63(1), 97–109.
- 744 Brew, K., Castellino, F. J., Vanaman, T. C., & Hill, R. L. (1970). The complete amino acid
745 sequence of bovine alpha-lactalbumin. *The Journal of biological chemistry*, 245(17),
746 4570–4582.
- 747 Burchard, W. (1992). Static and dynamic light scattering approaches to structure
748 determination of biopolymers. In *Laser Light Scattering in Biochemistry*: Cambridge:
749 *Royal Society of Chemistry*, 3-22.
- 750 Chaneton, L., Pérez Sáez, J. M., & Bussmann, L. E. (2011). Antimicrobial activity of bovine
751 β-lactoglobulin against mastitis-causing bacteria. *Journal of Dairy Science*, 94(1), 138–
752 145. doi:10.3168/jds.2010-3319
- 753 Cockerill, F. (2012). *Performance standards for antimicrobial susceptibility testing: Twenty-*
754 *second informational supplement. Clinical and laboratory standards institute: M100-S22*
755 *= v. 32, no. 3*. Wayne, PA: Clinical and Laboratory Standards Institute.
- 756 Das, K., & Kinsella, J. E. (1989). pH dependent emulsifying properties of beta-lactoglobulin.
757 *Journal of Dispersion Science and Technology*, 10(1), 77–102.

758 Dickinson, E. (1999). Adsorbed protein layers at fluid interfaces: interactions, structure and
759 surface rheology. *Colloids and Surfaces B: Biointerfaces*, 15(2), 161–176.
760 doi:10.1016/S0927-7765(99)00042-9

761 Dickinson, E. (2001). Milk protein interfacial layers and the relationship to emulsion stability
762 and rheology. *Colloids and Surfaces B: Biointerfaces*, 20(3), 197–210. doi:10.1016/S0927-
763 7765(00)00204-6

764 Engelhardt, K., Lexis, M., Gochev, G., Konnerth, C., Miller, R., Willenbacher, N., . . .
765 Braunschweig, B. (2013). pH Effects on the Molecular Structure of β -Lactoglobulin
766 Modified Air–Water Interfaces and Its Impact on Foam Rheology. *Langmuir*, 29(37),
767 11646–11655. doi:10.1021/la402729g

768 Fang, Y., & Dalgleish, D. G. (1997). Conformation of β -Lactoglobulin Studied by FTIR:
769 Effect of pH, Temperature, and Adsorption to the Oil–Water Interface. *Journal of Colloid
770 and Interface Science*, 196(2), 292–298. doi:10.1006/jcis.1997.5191

771 Fimognari, C., Turrini, E., Ferruzzi, L., Lenzi, M., & Hrelia, P. (2012). Natural
772 isothiocyanates: Genotoxic potential versus chemoprevention. *Mutation Research/Reviews
773 in Mutation Research*, 750(2), 107–131. doi:10.1016/j.mrrev.2011.12.001

774 Fogolari, F., Ragona, L., Zetta, L., Romagnoli, S., De Kruif, K. G., & Molinari, H. (1998).
775 Monomeric bovine β -lactoglobulin adopts a β -barrel fold at pH 2. *FEBS Letters*, 436(2),
776 149–154. doi:10.1016/S0014-5793(98)00936-3

777 Franke, D., Kikhney, A. G., & Svergun, D. I. (2012). Automated acquisition and analysis of
778 small angle X-ray scattering data. *Nuclear Instruments and Methods in Physics Research
779 Section A: Accelerators, Spectrometers, Detectors and Associated Equipment*, 689, 52–59.
780 doi:10.1016/j.nima.2012.06.008

781 Gao, J., Ma, R., Wang, W., Wang, N., Sasaki, R., Snyderman, D., . . . Ruan, K. (2014).
782 Automated NMR fragment based screening identified a novel interface blocker to the
783 LARG/RhoA complex. *PLoS ONE*, 9(2), e88098. doi:10.1371/journal.pone.0088098

784 Gaussier, H., Lavoie, M., & Subirade, M. (2003). Conformational changes of pediocin in an
785 aqueous medium monitored by Fourier transform infrared spectroscopy: a biological
786 implication. *International Journal of Biological Macromolecules*, 32(1–2), 1–9.
787 doi:10.1016/S0141-8130(03)00018-7

788 Gulzar, M., Lechevalier, V., Bouhallab, S., & Croguennec, T. (2012). The physicochemical
789 parameters during dry heating strongly influence the gelling properties of whey proteins.
790 *Journal of Food Engineering*, 112(4), 296–303. doi:10.1016/j.jfoodeng.2012.05.006

791 Halpin, M. I., & Richardson, T. (1985). Selected functionality changes of beta-lactoglobulin
792 upon esterification of side-chain carboxyl groups. *Journal of Dairy Science*, 68(12), 3189–
793 3198. doi:10.3168/jds.S0022-0302(85)81226-1

794 Hanschen, F. S., Brüggemann, N., Brodehl, A., Mewis, I., Schreiner, M., Rohn, S., & Kroh,
795 L. W. (2012). Characterization of Products from the Reaction of Glucosinolate-Derived
796 Isothiocyanates with Cysteine and Lysine Derivatives Formed in Either Model Systems or
797 Broccoli Sprouts. *J. Agric. Food Chem.*, 60(31), 7735–7745. doi:10.1021/jf301718g

798 Hawe, A., Sutter, M., & Jiskoot, W. (2007). Extrinsic Fluorescent Dyes as Tools for Protein
799 Characterization. *Pharmaceutical Research*, 25(7), 1487–1499. doi:10.1007/s11095-007-
800 9516-9

801 Hernández-Triana, M., Kroll, J., Proll, J., Noack, J., & Petzke, K. J. (1996). Benzyl-
802 isothiocyanate (BITC) decreases quality of egg white proteins in rats. *The Journal of
803 Nutritional Biochemistry*, 7(6), 322–326. doi:10.1016/0955-2863(96)00033-2

804 Hunt, J. A., & Dalgleish, D. G. (1994). Effect of pH on the stability and surface composition
805 of emulsions made with whey protein isolate. *J. Agric. Food Chem.*, *42*(10), 2131–2135.
806 doi:10.1021/jf00046a011

807 Ioannou, J. C., Donald, A. M., & Tromp, R. H. (2015). Characterising the secondary structure
808 changes occurring in high density systems of BLG dissolved in aqueous pH 3 buffer. *Food*
809 *Hydrocolloids*, *46*, 216–225. doi:10.1016/j.foodhyd.2014.12.027

810 Kataoka, M., Kuwajima, K., Tokunaga, F., & Goto, Y. (1997). Structural characterization of
811 the molten globule of alpha-lactalbumin by solution X-ray scattering. *Protein science : a*
812 *publication of the Protein Society*, *6*(2), 422–430. doi:10.1002/pro.5560060219

813 Kato, A. & Nakai, S. (1980). Hydrophobicity determination by a fluorescence probe method
814 and its correlation with surface properties of proteins. *Biochimica et Biophysica Acta*, *624*,
815 13–20. doi:10.1016/0005-2795(80)90220-2

816 Kawakishi, S., & Kaneko, T. (1987). Interaction of proteins with allyl isothiocyanate. *J.*
817 *Agric. Food Chem.*, *35*(1), 85–88. doi:10.1021/jf00073a020

818 Keppler, J. K., Martin, D., Garamus, V. M., & Schwarz, K. (2015). Differences in binding
819 behavior of (–)-epigallocatechin gallate to β -lactoglobulin heterodimers (AB) compared to
820 homodimers (A) and (B). *Journal of Molecular Recognition*, *28*(11), 656–666.
821 doi:10.1002/jmr.2480

822 Keppler, J. K., Koudelka, T., Palani, K., Stuhldreier, M. C., Temps, F., Tholey, A., &
823 Schwarz, K. (2014a). Characterization of the covalent binding of allyl isothiocyanate to β -
824 lactoglobulin by fluorescence quenching, equilibrium measurement, and mass
825 spectrometry. *Journal of biomolecular structure & dynamics*, *32*(7), 1103–1117.
826 doi:10.1080/07391102.2013.809605

827 Keppler, J.K, Koudelka, T., Palani, K., Tholey, A., & Schwarz, K. (2014b). Interaction of β -
828 Lactoglobulin with Small Hydrophobic Ligands - Influence of Covalent AITC
829 Modification on β -LG Tryptic Cleavage. *Food Biophysics*, 1-10. doi:10.1007/s11483-014-
830 9361-4

831 Keppler, J. K., Sönnichsen, F. D., Lorenzen, P.-C., & Schwarz, K. (2014c). Differences in
832 heat stability and ligand binding among β -lactoglobulin genetic variants A, B and C using
833 $(1)H$ NMR and fluorescence quenching. *Biochimica et biophysica acta*.
834 doi:10.1016/j.bbapap.2014.02.007

835 Kroll, J., Rawel, H., Kröck, R., Proll, J., & Schnaak, W. (1994). Interactions of
836 isothiocyanates with egg white proteins. *Food / Nahrung*, *38*(1), 53–60.
837 doi:10.1002/food.19940380110

838 Kroll, J., Noack, J., Rawel, H., Kroeck, R., & Proll, J. (1994). Chemical reactions of benzyl
839 isothiocyanate with egg-white protein fractions. *Journal of the Science of Food and*
840 *Agriculture*, *65*(3), 337–345. doi:10.1002/jsfa.2740650312

841 Lam, R. H., & Nickerson, M. (2014). The Effect of pH and Heat Pre-Treatments on the
842 Physicochemical and Emulsifying Properties of β -lactoglobulin. *Food Biophysics*, *9*(1), 20-
843 28. doi:10.1007/s11483-013-9313-4

844 Lam, Ricky S. H., & Nickerson, M. T. (2015). The effect of pH and temperature pre-
845 treatments on the physicochemical and emulsifying properties of whey protein isolate.
846 *LWT - Food Science and Technology*, *60*(1), 427–434. doi:10.1016/j.lwt.2014.07.031

847 Lamberto, I., Qin, H., Noberini, R., Premkumar, L., Bourgin, C., Riedl, S. J., . . . Pasquale, E.
848 B. (2012). Distinctive binding of three antagonistic peptides to the ephrin-binding pocket
849 of the EphA4 receptor. *The Biochemical journal*, *445*(1), 47–56. doi:10.1042/BJ20120408

850 Lestringant, P., Guri, A., Gülseren, İ., Relkin, P., & Corredig, M. (2014). Effect of Processing
851 on Physicochemical Characteristics and Bioefficacy of β -Lactoglobulin–Epigallocatechin-
852 3-gallate Complexes. *J. Agric. Food Chem.*, 62(33), 8357–8364. doi:10.1021/jf5029834

853 Litvinov, R. I., Faizullin, D. A., Zuev, Y. F., & Weisel, J. W. (2012). The α -Helix to β -Sheet
854 Transition in Stretched and Compressed Hydrated Fibrin Clots. *Biophysical journal*,
855 103(5), 1020–1027. doi:10.1016/j.bpj.2012.07.046

856 Luciano, F. B., & Holley, R. A. (2009). Enzymatic inhibition by allyl isothiocyanate and
857 factors affecting its antimicrobial action against *Escherichia coli* O157:H7. *International*
858 *Journal of Food Microbiology*, 131(2-3), 240–245. doi:10.1016/j.ijfoodmicro.2009.03.005

859 Majhi, P. R., Ganta, R. R., Vanam, R. P., Seyrek, E., Giger, K., & Dubin, P. L. (2006).
860 Electrostatically Driven Protein Aggregation: β -Lactoglobulin at Low Ionic Strength.
861 *Langmuir*, 22(22), 9150–9159. doi:10.1021/la053528w

862 Meersman, F., Smeller, L., & Heremans, K. (2002). Comparative Fourier transform infrared
863 spectroscopy study of cold-, pressure-, and heat-induced unfolding and aggregation of
864 myoglobin. *Biophysical journal*, 82(5), 2635–2644.

865 Moitzi, C., Donato, L., Schmitt, C., Bovetto, L., Gillies, G., & Stradner, A. (2011). Structure
866 of β -lactoglobulin microgels formed during heating as revealed by small-angle X-ray
867 scattering and light scattering. *Food Hydrocolloids*, 25(7), 1766–1774.
868 doi:10.1016/j.foodhyd.2011.03.020

869 Murthy, N. V. K. K., & Rao, M. S. N. (1986a). Interaction of allyl isothiocyanate with
870 mustard 12S protein. *Journal of agricultural and food chemistry*, 34(3), 448–452.
871 doi:10.1021/jf00069a017

872 Mushantaf, F., Blyth, J., & Templeton, M. R. (2012). The bactericidal effects of allyl
873 isothiocyanate in water. *Environmental technology*, 33(19-21), 2461–2465.
874 doi:10.1080/09593330.2012.671855

875 Muthukumarasamy, P., Han, J. H., & Holley, R. A. (2003). Bactericidal effects of
876 *Lactobacillus reuteri* and allyl isothiocyanate on *Escherichia coli* O157:H7 in refrigerated
877 ground beef. *Journal of food protection*, 66(11), 2038–2044.

878 Nakamura, T., Kawai, Y., Kitamoto, N., Osawa, T., & Kato, Y. (2009). Covalent modification
879 of lysine residues by allyl isothiocyanate in physiological conditions: plausible
880 transformation of isothiocyanate from thiol to amine. *Chemical research in toxicology*,
881 22(3), 536–542. doi:10.1021/tx8003906

882 Palani, K., Harbaum-Piayda, B., Meske, D., Keppler, J. K., Bockelmann, W., Heller, K. J., &
883 Schwarz, K. (2016). Influence of fermentation on glucosinolates and glucobrassicin
884 degradation products in sauerkraut. *Food Chemistry*, 190, 755–762.
885 doi:10.1016/j.foodchem.2015.06.012

886 Palladino, P., Portella, L., Colonna, G., Raucci, R., Saviano, G., Rossi, F., . . . Costantini, S.
887 (2012). The N-terminal region of CXCL11 as structural template for CXCR3 molecular
888 recognition: synthesis, conformational analysis, and binding studies. *Chemical Biology &*
889 *Drug Design*, 80(2), 254–265. doi:10.1111/j.1747-0285.2012.01397.x

890 Pan, B., Cui, D., He, R., Gao, F., & Zhang, Y. (2006). Covalent attachment of quantum dot on
891 carbon nanotubes. *Chemical Physics Letters*, 417(4–6), 419–424.
892 doi:10.1016/j.cplett.2005.10.044

893 Pan, Y., Shiell, B., Wan, J., Coventry, M. J., Michalski, W. P., Lee, A., & Roginski, H.
894 (2007). The molecular characterisation and antimicrobial properties of amidated bovine β -
895 lactoglobulin. *International Dairy Journal*, 17(12), 1450–1459.
896 doi:10.1016/j.idairyj.2007.04.006

897

898 Panick, G., Malessa, R., & Winter, R. (1999). Differences between the pressure- and
899 temperature-induced denaturation and aggregation of beta-lactoglobulin A, B, and AB
900 monitored by FT-IR spectroscopy and small-angle X-ray scattering. *Biochemistry*, 38(20),
901 6512–6519. doi:10.1021/bi982825f

902 Pelton, J. T., & McLean, L. R. (2000). Spectroscopic Methods for Analysis of Protein
903 Secondary Structure. *Analytical biochemistry*, 277(2), 167–176.
904 doi:10.1006/abio.1999.4320

905 Qi, X. L., Holt, C., McNulty, D., Clarke, D. T., Brownlow, S., & Jones, G. R. (1997). Effect
906 of temperature on the secondary structure of beta-lactoglobulin at pH 6.7, as determined by
907 CD and IR spectroscopy: a test of the molten globule hypothesis. *Biochemical Journal*,
908 324(Pt 1), 341–346. <http://www.ncbi.nlm.nih.gov/pmc/articles/PMC1218435/>

909 Rade-Kukic, K., Schmitt, C., & Rawel, H. M. (2011). Formation of conjugates between
910 [beta]-lactoglobulin and allyl isothiocyanate: Effect on protein heat aggregation, foaming
911 and emulsifying properties: Food Colloids 2010: On the Road from Interfaces to
912 Consumers. *Food Hydrocolloids*, 25(4), 694–706.
913 [http://www.sciencedirect.com/science/article/B6VP9-511C040-](http://www.sciencedirect.com/science/article/B6VP9-511C040-1/2/6df8f8f29df1961cbf402e8139dcfe09)
914 [1/2/6df8f8f29df1961cbf402e8139dcfe09](http://www.sciencedirect.com/science/article/B6VP9-511C040-1/2/6df8f8f29df1961cbf402e8139dcfe09)

915 Rawel, H. M., Kroll, J., & Schröder, I. (1998). In Vitro Enzymatic Digestion of Benzyl- and
916 Phenylisothiocyanate-Derivatized Food Proteins. *J. Agric. Food Chem.*, 46(12), 5103–
917 5109. doi:10.1021/jf980244r

918 Reinstädler, D., Fabian, H., Backmann, J., & Naumann, D. (1996). Refolding of thermally and
919 urea-denatured ribonuclease A monitored by time-resolved FTIR spectroscopy.
920 *Biochemistry*, 35(49), 15822–15830.

921 Rühls, P. A., Affolter, C., Windhab, E. J., & Fischer, P. (2013). Shear and dilatational linear
922 and nonlinear subphase controlled interfacial rheology of beta-lactoglobulin fibrils and
923 their derivatives. *Journal of Rheology*, 57(3), 1003–1022. Retrieved from
924 <http://dx.doi.org/10.1122/1.4802051>

925 Sagis, L. M. C., & Scholten, E. (2014). Complex interfaces in food: Structure and mechanical
926 properties. *Trends in Food Science & Technology*, 37(1), 59–71.
927 doi:10.1016/j.tifs.2014.02.009

928 Sawyer, L., & Kontopidis, G. (2000). The core lipocalin, bovine [beta]-lactoglobulin.
929 *Biochimica et Biophysica Acta (BBA) - Protein Structure and Molecular Enzymology*,
930 1482(1-2), 136–148. Retrieved from [http://www.sciencedirect.com/science/article/B6T21-](http://www.sciencedirect.com/science/article/B6T21-41HHN9X-H/2/cc73232c1860ad921ea3cf92a6b4795e)
931 [41HHN9X-H/2/cc73232c1860ad921ea3cf92a6b4795e](http://www.sciencedirect.com/science/article/B6T21-41HHN9X-H/2/cc73232c1860ad921ea3cf92a6b4795e)

932 Sitohy, M., Chobert, J. M., & Haertlé, T. (1995). Phosphorylation of β -Lactoglobulin under
933 Mild Conditions. *Journal of Agricultural and Food Chemistry*, 43(1), 59–62. DOI:
934 10.1021/jf00049a012

935 Sitohy, M., Chobert, J. M., & Haertlé, T. (2001). Improvement of solubility and of
936 emulsifying properties of milk proteins at acid pHs by esterification. *Die Nahrung*, 45(2),
937 87–93. doi:10.1002/1521-3803(20010401)45:2<87::AID-FOOD87>3.0.CO;2-Z

938 Swart, P.J., Kuipers, M.E., Smit, C., Pauwels, R., De Béthune, M.P., De Clercq, E., Meijer,
939 D.K.F. & Huisman, J.G. (2009). Antiviral Effects of Milk Proteins: Acylation results in
940 polyanionic compounds with potent activity against human immunodeficiency virus types
941 1 and 2 in vitro. *AIDS Research and Human Retroviruses*, 12(9): 769-775.
942 doi:10.1089/aid.1996.12.769.

943 Tande, B. M., Wagner, N. J., Mackay, M. E., Hawker, C. J., & Jeong, M. (2001).
944 Viscosimetric, Hydrodynamic, and Conformational Properties of Dendrimers and
945 Dendrons. *Macromolecules*, 34(24), 8580–8585. doi:10.1021/ma011265g

946 Tomczyn´ska-Mleko, M., Kamysz, E., Sikorska, E., Puchalski, C., Mleko, S., Ozimek, L., . . .
947 Wesołowska-Trojanowska, M. (2014). Changes of secondary structure and surface tension
948 of whey protein isolate dispersions upon pH and temperature. *Czech Journal of Food*
949 *Sciences*, 32(1), 82-89.

950 van Kempen, S. E., Schols, H. A., van der Linden E, & Sagis, L. M. (2013). Non-linear
951 surface dilatational rheology as a tool for understanding microstructures of air/water
952 interfaces stabilized by oligofructose fatty acid esters. *Soft Matter*, 9(40), 9579–9592.

953 Vega-Lugo, A.-C., & Lim, L.-T. (2009). Controlled release of allyl isothiocyanate using soy
954 protein and poly(lactic acid) electrospun fibers. *Food Research International*, 42(8), 933–
955 940. doi:10.1016/j.foodres.2009.05.005

956 Verheul, M., Pedersen, J. S., Roefs, S. P. F. M., & Kruif, K. G. de. (1999). Association
957 behavior of native β -lactoglobulin. *Biopolymers*, 49(1), 11–20. Retrieved from
958 [http://dx.doi.org/10.1002/\(SICI\)1097-0282\(199901\)49:1<11::AID-BIP2>3.0.CO;2-1](http://dx.doi.org/10.1002/(SICI)1097-0282(199901)49:1<11::AID-BIP2>3.0.CO;2-1)

959 Wilde, S. C., Keppler, J. K., Palani, K., & Schwarz, K. (2016a). beta-Lactoglobulin as
960 nanotransporter--Part I: Binding of organosulfur compounds. *Food Chemistry*, 197 (Part
961 A), 1015–1021. doi:10.1016/j.foodchem.2015.11.010

962 Wilde, S. C., Keppler, J. K., Palani, K., & Schwarz, K. (2016b). β -Lactoglobulin as
963 nanotransporter for allicin: Sensory properties and applicability in food. *Food Chemistry*,
964 199, 667–674. doi:10.1016/j.foodchem.2015.12.055

965 Wilde, S. C., Treitz, C., Keppler, J. K., Koudelka, T., Palani, K., Tholey, A., . . . Schwarz, K.
966 (2016c). β -Lactoglobulin as nanotransporter – Part II: Characterization of the covalent
967 protein modification by allicin and diallyl disulfide. *Food Chemistry*, 197, Part A, 1022–
968 1029. doi:10.1016/j.foodchem.2015.11.011

969 Zhai, J., Wooster, T. J., Hoffmann, S. V., Lee, T.-H., Augustin, M. A., & Aguilar, M.-I.
970 (2011). Structural rearrangement of β -lactoglobulin at different oil-water interfaces and its
971 effect on emulsion stability. *Langmuir : the ACS journal of surfaces and colloids*, 27(15),
972 9227–9236. doi:10.1021/la201483y

973

974

975

976

977

978

979

980

981

982

983

984

985

986

987

988

989

990

991

992

993

994